VOL. 14, NO. 18, SEPTEMBER 2019 ISSN 1819-6608
ARPN Journal of Engineering and Applied Sciences

www.arpnjournals.com

EXPERIMENTAL STUDY OF DEFORMATION AND PORE WATER PRESSURE FOR EMBANKMENT ON SOFT SOIL USING RAPID IMPACT COMPACTION

Arifin B, Lawalenna Samang, Tri Harianto and Achmad Bakri Muhiddin
Civil Engineering Department, Hasanuddin University, Indonesia
E-Mail: arifin_beddu@yahoo.com

ABSTRACT

This study was conducted to analyze the deformation behavior and increases of pore water pressure on an embankment construction on the clay soil layer which is compacted using the Rapid Impact Compaction (RIC) Method. In this study, an equipment model was used that can simulate the RIC method which was electro-mechanically controlled at frequency of 30-40 blows per minute. The compaction test mold has a diameter of 80 cm and height of 120 cm, tested clay layer has a thickness of 80 cm and the sand-and-gravel embankment has a thickness of 30 cm. The clay layer was attached with pore pressure cell and earth pressure cell. An ultra-sonic sensor and a dial gauge were put on the surface. The compaction process with RIC was carried out up to 300 blows using a 45kg impact mass, falling height of 15 cm, impact base diameter(B) of 30 cm. The results showed the achievement of 90% of maximum vertical deformation on the impact foot occurred at 175 blows and heaving surfaces occurred at a distance of 0.80B from the center of the impact base, while at the 300 blows, the heaving surfaces distance was 0.90B. The analysis showed the generation of excess pore water pressure following the phenomenon of undrained conditions in the cyclic dynamic loading, where there was a very fast increases of pore water pressure at the 55 first of blows of the initial stage of compaction and then the increase rate reduced until reaching the constant line after the 175 blows.

Keywords:rapid impact compaction, embankment, clay, pore water pressure, undrained.

1. INTRODUCTION

The construction of an embankment on soft soil can be found in almost all development sectors such as highways, railroads, airports, ports, residential areas and offices [1][2]. In its implementation, an embankment on soft soil are faced with common problems, such as excessive deformation in the form of differential settlement and low bearing capacity [3][4][5]. Differential settlementis characterized by a non-uniform settlement between the longitudinal direction of the transverse direction of the part which high load repetition, while the low bearing capacity causes a long-term settlement in the surface of the embankment even to a lower level than the existing ground surfaces [6][7]. This condition is certainly not expected because it will require maintenance costs for the embankment to maintain its operations.

There have been a number of technological and methodological innovations implemented to minimize the problems that arise in constructing an embankment on soft soil, which can be divided according to innovation to strengthen the embankment structures and innovations to the soft soil layer. [4][8][9][10][11][12][13]. It has been common to improve the embankment structures by processing or improving on the embankment materials, with or without reinforcement, as well as the selection of dynamic compaction methods.

One of the dynamic compaction methods for thick embankment known today includes *Rapid Impact Compaction*. This method is dynamic soil compaction with the concept of Low Energy Dynamic Compaction, [14][15][16]. The main equipment of Rapid Impact Compaction is a mass of hammer dropped from a certain height. What distinguishes this method from Dynamic Compaction is the use of lighter hammer masses, lower free-fall but with a higher impact frequency of 30-40 blows per minute, so the total cumulative energy produced in the RIC method is greater than the Dynamic Compaction (DC) in the same time unit [15].

Operationally, Rapid Impact Compaction will have the effect of cyclic loads resulting from impact momentum and force on the impact base on the embankment surface, this not only has an effect on increasing density but also results of pore pressure generation and soil grains reposition, [3][17][18]. In the saturated clay layer, dynamic compaction will generate excess pore pressure, especially for undrained conditions, while in partially drained conditions there will be generate and dissipation of pore water pressure simultaneously [19]. Cyclic loading under undrained conditions causes effective stress reduction, when drainage occurs after cyclic loading, excess pore pressure will be lost and effective stress reaches the initial value before cyclic loading restarts.

The amount of internal excess pore pressure generated during cyclic loading is partly influenced by the history and dissipation of cyclic stresses and will be different from that obtained from the cyclic loading of undrained conditions. In both the undrained and partially drained conditions the increase of pore pressure is rapidly produced in the early stages of cyclic loading, the peak of the pore pressure increase curve and its dissipation can be an indication of whether the cyclic loading carried out results in the effects of drained or partially drained conditions [20].

Thus, this study aimed to analyze the pattern of deformation of the construction of an embankment on soft

soil and to analyze the increase of pore water pressure in the clay layer during compaction using the Rapid Impact Compaction method through an experimental model test in the laboratory.

2. TESTING MATERIALS AND EQUIPMENT

2.1 Clay Soil

The soil used in the study was local soil around the campus of the Faculty of Engineering of Hasanuddin University in Gowa Regency, South Sulawesi, which was excavated at a depth of 1 - 2m. The natural physical properties of soil consist of sand fraction of 36.62%, silt 27.55%, clay 35.83% with specific gravity of 2.74, plastic limit of 6.01%, liquid limit of 23.71%, and plasticity index of 17.7% of soil samples which were classified as (CL-ML) according to the USCS soil classification system.

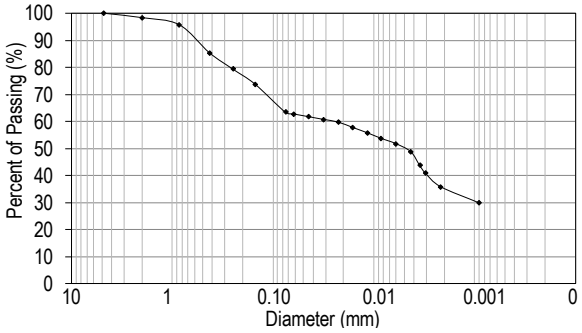

Figure-1. Soil grain size distribution.

2.2 Embankment Materials

The sand-and-gravel layer has loose density of 12.40 kN/m^3, natural water content of 53.40%, specific gravity of 2.65, maximum dry weight of proctor compaction of 20.4 kN/m^3 at optimum water content of 7.92%.

2.3 Equipment and Instruments

2.3.1 Repeated Impact Compaction Equipment

In this study, there was a laboratory scale model of Repeated Impact Load compaction developed, based on pneumatics with actuator control from a microcontroller. The main components of the equipment consist of an air compressor; solenoid valve, controller panel for actuation, and double acting piston as is shown in Figure-2.

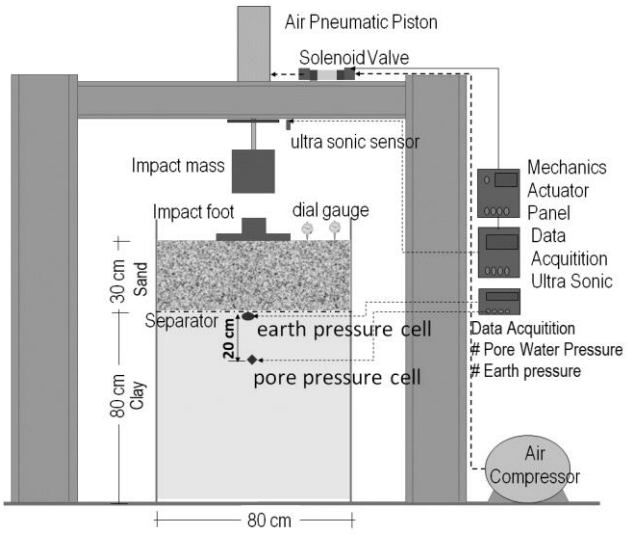

Figure-2. The experimental set up of RIC Model.

2.3.2 Impact Mass

In order to generate the impact energy, there was impact mass made of steel used weighing about 45kg linked to the ends of pneumatic cylinder rods as shown in Figure-3.

The impact mass can be dropped at a height according to the height setting on the control panel, which is 10-25 cm, and the pneumatic capacity can be varied up to 150 kg as necessary. For the compaction process, the mold is equipped with impact foot which has a diameter of 30cm.

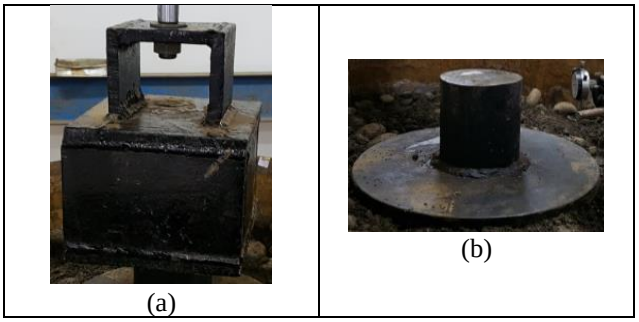

Figure-3. Impact mass (a) and impact foot (b).

2.3.3 Testing Mold

The testing mold used with a diameter of 80cm and height 120cm, which is waterproof coated.

Figure-4. Testing Mould Equipment.

2.3.4 Measurement Instrument

There were two types of pressure cells used based on their functions, namely pore water pressure cell and earth pressure cell. Pore-water pressure cell, based on the specifications, was specifically designed to effectively measure pore-water pressure around the test model in the clay layer, while the earth pressure cell can monitor changes in soil pressure. Both of these pressure cells can function effectively both in static and dynamic conditions. As for the observation of vertical and surface deformation, an ultrasonic sensor was used which was directed at the impact base and the dial gauge placed on the pile surface.

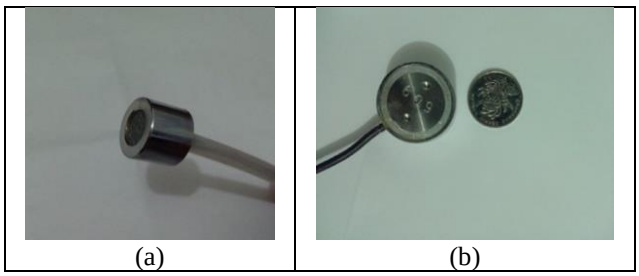

Figure-5. Measurement instrument, Pore-water pressure cell (a), earth pressure cell(b)

3. EXPERIMENTAL PROGRAM

3.1 Testing Model Scheme

The bottom layer of the test container was filled with 80 cm thick clay, and 30 cm embankment layered on the clay surface. The boundary between clay and sand-and-gravel play was installed for separator material, and the test container was conditioned without drainage at the bottom of the clay so that the test mold became impermeable. The pore water pressure cell was installed at a depth of 20 cm from the surface of the clay, while the earth pressure cell was installed on the surface of the clay, and the compaction base or foot hammer was placed on the center of the container. Figure-6.

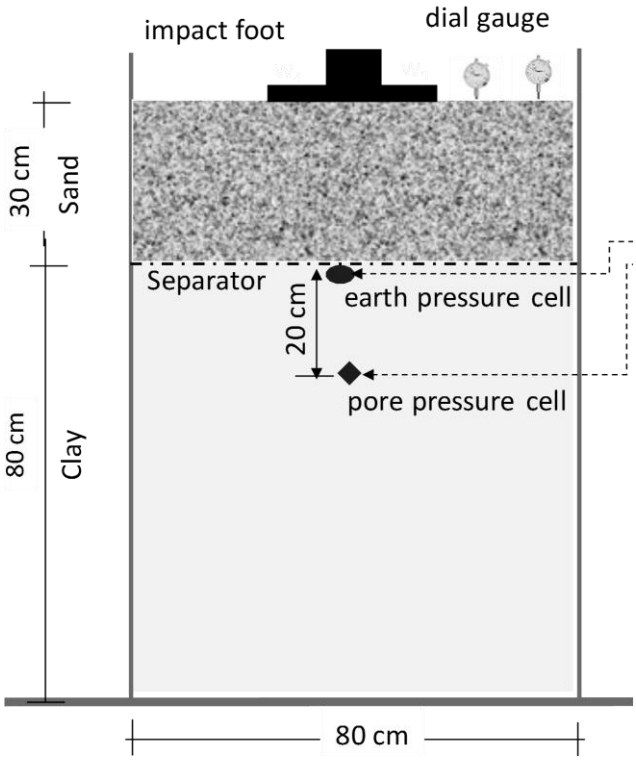

Figure-6. The testing model set up.

3.2 Monitoring of Surface deformation

Observation of surface deformation was conducted by placing a dial gauge at a distance of 21 cm and 32 cm, respectively, from the center of the impact foot, while the ultrasonic sensor to measure vertical deformation during compaction was highlighted at the edge of the impact foot.

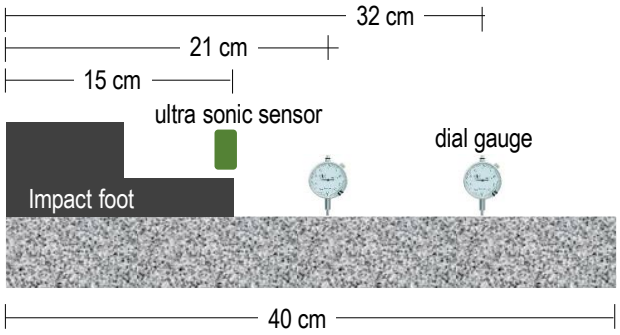

Figure-7. Placement of tool and monitoring point of deformation for horizontal direction surface.

3.3 Testing Condition and Soil Sample

Before the placement of the sand-and-gravel as embankment layer, there was pre-consolidation carried out first by the reconstitution method in the clay layer. The test was carried out in conditions of saturated water clay

with Sr = 100%, for water content 79.81%, volume weight 15.23 kN/m^3, by adjusting the location of the soil taking depth of 1.0-2.0 m, the pre-consolidation load considered was 15 kN/m^2, and the reconstitution process was carried out for 3x24 hours until the settlement was no longer significant. After the reconstitution process completed, the next step was the placement of the sand-and-gravel embankment layer over the clay layer.

3.4 Compaction Processes

The compaction process was carried out by dropping the hammer mass of Rapid Impact Compaction test on the impact foot which has been placed on the surface of the test mold, as the impact mass was repeatedly dropped N cycles for appropriate height, and all stages of the compaction process were controlled electronically from the actuator control panel. The equipment model can be set at several free-fall heights and impact mass types, but this study was limited to each of the free-fall height variable tested of h = 15cm, and 45kg impact mass.

(a)(b)

(c)(d)

Figure-8. The sequence of the compaction process test model, a. Mold that have been filled with embankment materials and clay. b. Placement of impact foot and observation point c, d Compaction processes.

4. RESULTS AND DISCUSSIONS

4.1 Compaction Criteria

The determination of the number of ideal blow related to the RIC method to stop compaction was carried out by adopting the Asaoka method using data from observations on the relationship of the magnitude of vertical deformation, δ_N, which corresponds to the number of blows, N as shown in Figure-9.

The equation for the line resulted from vertical deformation data plotting of δ_N towards δ_{N-1} in Figure-8 meets the Equation-1.

$$\delta_N = 0.661 + 0.987.\delta_{N-1} \quad (1)$$

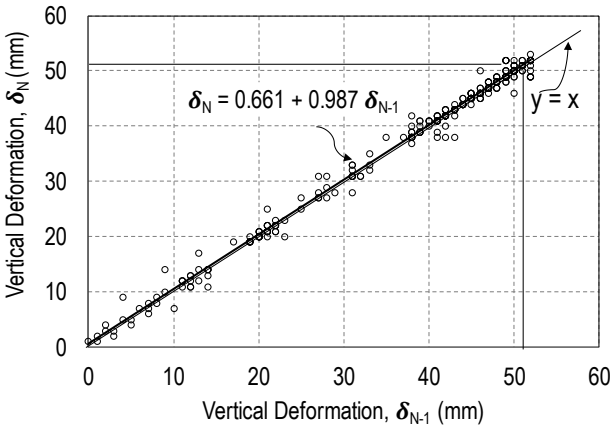

Figure-9. Correlation of vertical deformation δ_{N-1} and δ_N using Asaoka Method.

Based on Equation-1, it was obtained $\delta_{N(max)}$ of 50.85mm, in this case if the final set used the criteria 90% $\delta_{N(max)}$ then the amount of vertical deformation is 45.76mm. The final set corresponds to the number of 175 blows as N_{90} or 58.33% of the total number of blows until the maximum reduction observed in 300 blows. This is clearly shown in Figure-10.

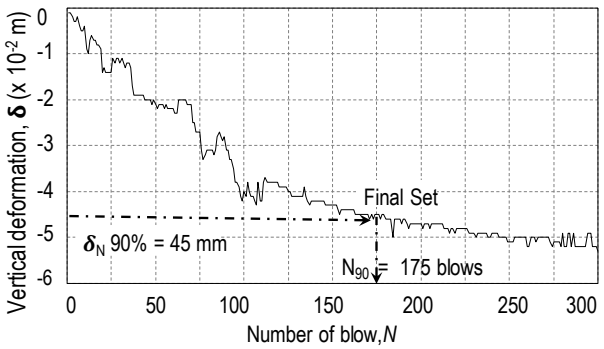

Figure-10. Determination of final set of vertical deformation according to $\delta_{N(90\%)}$ and N_{90}.

4.2 Surface Deformation

As shown in Figure-11, during the compaction process using RIC, the data taken at the 175 blows shows vertical deformation occurring at 4.5cm, followed by the occur of heaving surface deformation with the starting point at a distance of 23cm from the center of the impact base. The dial displacement observation point indicates the amount of heaving of 0.5 cm. Meanwhile, at the last impact of 300 impacts as shown in Figure-12, vertical deformation increases to 5.4 cm, which was followed by moving the starting point of heaving to 27 cm and the amount of heaving of 0.8 cm.

The data indicate that the surface deformation in the form of heaving magnitude and distance are influenced by the amount of vertical deformation caused by the presence of a number of blows on the base of the contact area. Figure-13 and Figure-14 show the tendency of surface deformation that occurs around the impact base contact area, if it is connected with the final criteria of the compaction set at 175 blows, the starting point of heaving is 23 cm or 0.8 B and and 27 cm or 0.9B at 300 blows, where in this case, B is the impact foot diameter of 30cm.

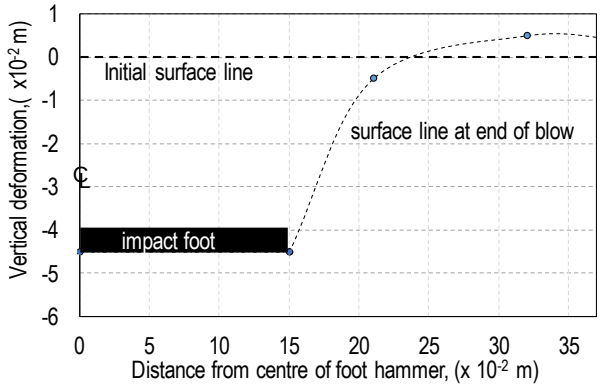

Figure-11. Vertical and Surface Deformation at the 175 blows.

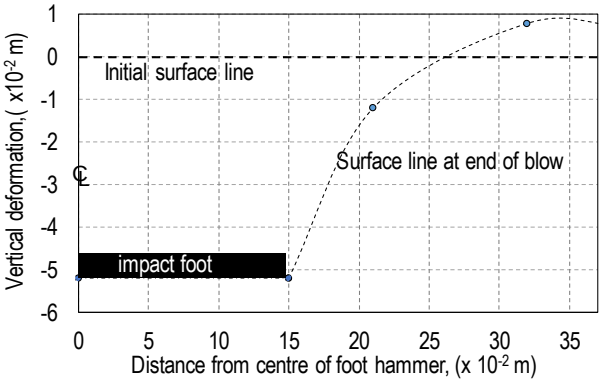

Figure-12. Vertical and Surface Deformation at the 300 blows.

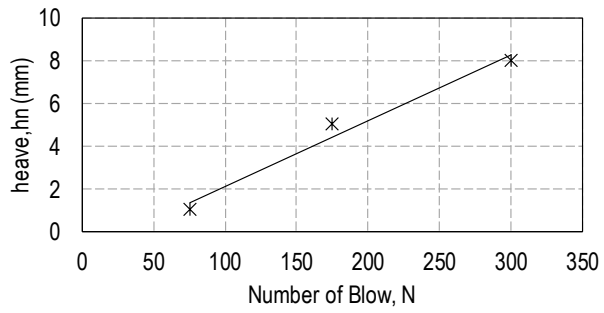

Figure-13. The correlation of surface deformation magnitude on the number of blows.

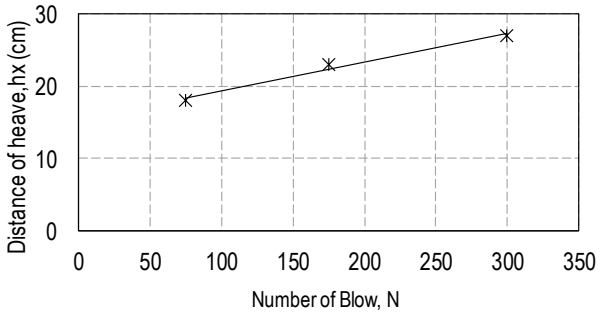

Figure-14. The correlation of surface deformation distance on the number of blows.

4.3 Generation of Excess Pore Water Pressure

As in previous studies, when the saturated soil is subjected to dynamic loads under undrained conditions with medium to large quantities, in line with the increase in the number of impact cycles, N, will generate a pore water pressure of Δu. In this study, the results of the analysis show that the pore pressure increases rapidly at the initial of the compaction stage and then the rate increases more slow than the previous phase until the stability of the increase is reached, as it can be observed that the increase of pore water pressure is in line with the amount of deformation that occurs until the blow reaches N cycles as shown in Figure-15.

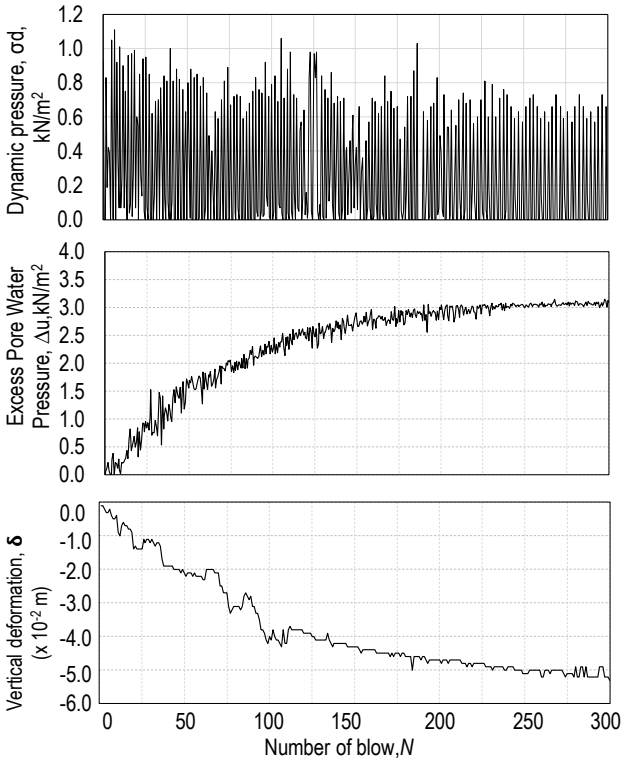

Figure-15. The correlation of the number of blows, N, on dynamic pressure, excess of pore water, and vertical deformation.

The greatest generation of excess pore water pressure occurred in the first of 55 blows or 18.3% of the

total number of blows analyzed, the magnitude of the increase is 1.65 kN/m^2 or 53.23% of the maximum pore pressure of 3.10 kN/m^2, the rate of increase of pore water pressure is 0.030 (kN/m^2/blow), this phase is a linear zone. Furthermore, in the next 120 blows, the increase of pore water pressure is 1.15 kN/m2, where in this zone there is a deceleration of pore pressure increase as compared to the previous zone, the rate of increase of pore water pressure in this zone is only 0.01 kN/m^2/blow, the increase of pore water in this stage is 37.10%, so this zone can be categorized as a deceleration stage.

Table-1. The increase of excess pore water pressure.

Phase	Number of blow,ΔN		Increase of EPWP, Δu	Percent of EPWP Increase	Ratio Δu/ΔN
	N,	(%)	(kN/m^2)	(%)	(kN/m^2/blow)
Linier	55	18.3	1.65	53.23	0.030
Decelaration	120	40.0	1.15	37.10	0.010
Stable	125	41.7	0.30	9.68	0.002

Based on Figure-16, it can be seen clearly that the third zone is a stable stage for the number of 125 blows, as the increase in pore water pressure is only 0.30 kN/m^2 and the increase in pore-water pressure in this zone is only 0.002 kN/m^2/blow, which give an increase in pore-water in this stage by 9.68%. In the third drainage analysis, the third zone is a pore pressure degradation if cyclic or compaction is stopped at this stage.

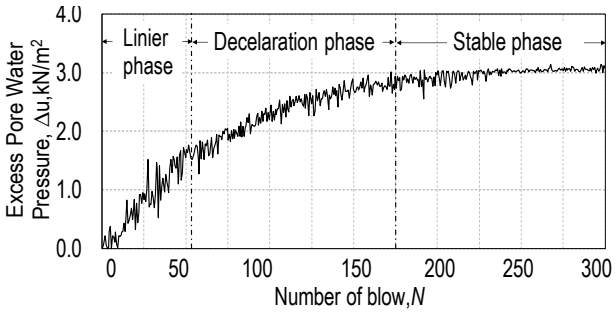

Figure-16. The generation patterns of excess pore pressure.

Overall, the pore water pressure increase curve shows an undrained condition during the compaction cycle, this is suitable with previous studies [18][19], where the curvature shows that the rate of increase in pore pressure is rapidly generated in the early stages of cyclic loading under undrained conditions.

CONCLUSIONS

The achievement of 90% of maximum vertical deformation at the base of the impact base contact area tends to occur after 175 blows or more than 50% of the total impacts observed. Vertical deformation is followed by the tendency of heaving around the impact base with distance and width affected by the number of blows.

The RIC model test over the saturated clay soil found that the deformation and increases of pore-water pressure that occur follows the phenomenon of undrained conditions in cyclic dynamic loading where the curvature shows that the increase in pore pressure is rapidly generated in the initial compaction process.

ACKNOWLEDGMENT

The authors are thankful to the Directorate General of Higher Education of the Ministry of Research, Technology, and Higher Education for the scholarship grant in completing this study through the 2015 Domestic Post-Graduate Scholarship (BPPDN).

REFERENCES

[1] Y. Guan-Bao, Z. Zhen, H. Jie, X. Hao-Feng, H. Mao-Song and X. Pei-Lin.2013.Performance Evaluation of an Embankment on Soft Soil Improved by Deep Mixed Columns and Prefabricated Vertical Drains, J. Perform. Constr. Facil.27(5): 614-623.

[2] M. W. Bo, A. Arulrajah, P. Sukmak and S. Horpibulsuk. 2015. Mineralogy and geotechnical properties of Singapore marine clay at Changi. Soils Found. 55(3): 600-613.

[3] K. M. Briggs, F. A. Loveridge and S. Glendinning. 2016. Failures in transport infrastructure embankments. J. Eng. Geol. 55(3): 600-613.

[4] E. Cascone and G. Biondi. 2013. A case study on soil settlements induced by preloading and vertical drains. J. Geotext and Geomembranes. 38: 51-67.

[5] X. Weng and W. Wang. 2011. Influence of differential settlement on pavement structure of widened roads based on large-scale model test. Journal of Rock and Mech. Geotech. Eng.3(1): 90-96.

[6] J. Chen, L. Fu, A. a Ungar and X. Zhao. 2009. Solving the Problems of Differential Settlement of Pavement Structures in the Bangkok Area. Geo Hunan International Conference ASCE. 189: 180-185.

[7] A. S. Balasubramaniam, H. Cai, D. Zhu, C. Surarak and E. Y. N. Oh. 2010. Settlements of embankments in soft soils. Geotech. Eng. J. SEAGS AGSSEA. 41(2): 1-19.

[8] T. Harianto, S Hayashi, YJ Du, D Suetsugu. 2008. Effects of fiber additives on the desiccation crack behavior of the compacted Akaboku soil as a material for landfill cover barrier,Water, air, and soil pollution. 194(1-4): 141-149.

[9] Sofwan, L. Samang, T. Harianto and A. B. Muhiddin. 2018. Experimental Study of Clay Stabilization with Quick Lime Activated by Gum Rosin and Iron Oxide. Int. J. Civ. Eng. 5(7): 17-21.

[10] Y. T. Todingrara, M. W. Tjaronge, T. Harianto, and M. Ramli. 2017. Performance of Laterite Soil Stabilized with Lime and Cement as a Road Foundation. Int. J. Appl. Eng. Res.12(14): 4699-4707.

[11] H. L. Liu, C. W. W. Ng and K. Fei. 2007. Performance of a Geogrid-Reinforced and Pile-Supported Highway Embankment over Soft Clay: Case Study. J. Geotech and Geoenvironmental Eng.133(12): 1483-1493.

[12] J. F. Chen, L. Y. Li, J. F. Xue and S. Z. Feng.2015 Failure mechanism of geosynthetic-encased stone columns in soft soils under embankment. J. Geotext and Geomembranes. 43(5): 424-431.

[13] G. K. Branch, G. Kavoos and A. Branch.2016. Evaluating the Behavior of a Column-Supported Embankment Founded on Soft Ground. Geo-China 2016 GSP 258 68,pp. 68-76.

[14] M. Parvizi.2009. Soil response to surface impact loads during low energy dynamic compaction, J. Appl. Sci.9(11): 2088-2096.

[15] P. J. Becker. 2011. Assessment of rapid impact compaction for transportation infrastructure applications, Graduate Theses and Dissertations. Paper 10261. Iowa State University.

[16] M. M.Mohammed, H. Roslan and S. Firas. 2013. Assessmen of rapid impact compaction in ground improvement from in-situ testing. J. Cent. South Univ. 20: 786-790.

[17] B. Hamidi, H. Nikraz and S. Varaksin. 2009. A Review on Impact Oriented Ground Improvement. https://australiangeomechanics.org/wpcontent/uploads/2015/03/44_2_3.pdf.

[18] F. Falkner, C. Adam, I. Paulmichl, D. Adam and J. Fürpass. 2010. Rapid Impact Compaction for Middle-Deep Improvement of the Ground - Numerical and Experimental Investigations. From Res. to Des. Eur. Pract., no. June, pp. 2-11.

[19] J. Ni, B. Indraratna, X. Geng and J. Philip. 2013. Radial consolidation of soft soil under cyclic loads. Comput. Geotech. 50: 1-5.

[20] Sakai. A, Samang. L, Miura.N. 2003. Partially Drained Cyclic Behaviour and Its Application to The Settlement of a Low Embankment Road on Silty Clay. Soils Found. 43(1): 33-46.